J. Fluid Mech. (1983), *vol.* 132, *pp.* 1–23
Printed in Great Britain

Effects of slowly varying depth and current on the evolution of a Stokes wavepacket

By FRANÇOIS-MARC TURPIN, CHAKIB BENMOUSSA AND CHIANG C. MEI
Department of Civil Engineering, Massachusetts Institute of Technology

(Received 10 August 1982 and in revised form 20 January 1983)

We consider the effects of slowly varying depth and current on the evolution of a packet of Stokes waves. The lengthscale of one-dimensional depth variation is assumed to be much greater than that of the wave envelope, and the direction of the current is perpendicular to the depth contours. By the method of multiple scales, the wave envelope is found to satisfy a cubic Schrödinger equation with slowly varying coefficients The criterion of spatial instability to small sidebands is extended. Numerical integration shows that the nonlinear evolution of a wavepacket is directly related to the instability parameter, which depends strongly on the current and depth variation. The heuristic hypothesis of Djordjevic & Redekopp on the soliton evolution over a slope in the absence of current is assessed.

1. Introduction

The evolution of weakly nonlinear surface waves on non-uniform depth is important to the understanding of coastal wave climate. For very long waves in shallow water, numerical integration of Boussinesq equations has revealed that a soliton from deeper water is first distorted while climbing the slope, and then forced to emit several solitons along the shelf of smaller but constant depth (Madsen & Mei 1969). Approximations for very gentle slopes have led to a simpler Korteweg–de Vries (KdV) equation with variable coefficients. By suitable approximation over the slope and the use of the exact solution by inverse-scattering theory to subsequent events on the shelf, soliton fission has been analytically confirmed (for other related papers see Tappert & Zabusky 1971; Johnson 1973; Ono 1974; Miles 1980).

It is well known that the evolution of a long envelope of short surface waves is also characterized by the competition between nonlinearity and dispersion. In deep water or finite but constant depth, a wavepacket can emit bound solitons which do not separate but interact to exhibit recurrence. These interesting features can be inferred from the exact solution of Zakharov & Shabat (1972) and have been ellucidated by Satsuma & Yajima (1974) and Yuen & Lake (1980), who surveyed both theories and experiments. The effects of variable depth have been studied by Djordjevic & Redekopp (1978), who deduced a cubic Schrödinger equation with variable coefficients for bottom slopes that are much less than the slope of the envelope. They predict that a soliton envelope can undergo fission only if it propagates into deeper water. By heuristic assumptions for the evolution along the slope, they also estimate the number of solitons emitted after a single soliton descends from a shallower shelf.

In this paper we extend the study of Djordjevic & Redekopp by incorporating the

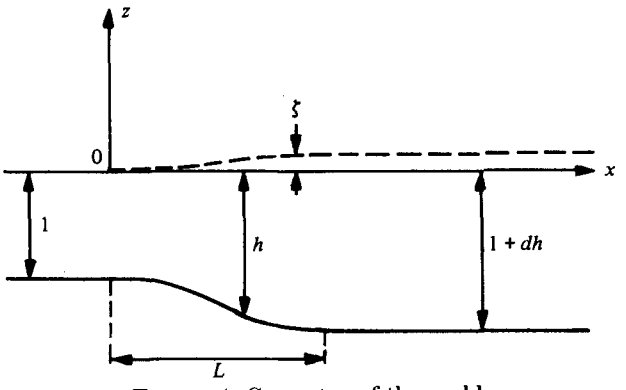

FIGURE 1. Geometry of the problem.

effect of a current whose presence is known to be important to infinitesimal waves. The current is allowed to be as strong as the phase velocity of the waves, and varies in space in accordance with the changing depth. A cubic Schrödinger equation is also found for the wave envelope; the coefficients in the equation now depend on the current. We first show that the shoaling of an infinite train of Stokes waves obey the same formula as the infinitesimal waves, this fact corresponds to the known result that a shoaling solitary wave obeys Green's law. We then show that the instability criterion of Benjamin & Feir (1967) for uniform depth can be extended to the shoaling Stokes waves on slowly varying depth and current. Results of a numerical study are then discussed. For pure depth variation without current, our results confirm Djordjevic & Redekopp in that fission is possible only if a soliton propagates into a region of greater depth; but their hypothesis on the events along the slope is not quantitatively supported. While a subcritical current along the wave gives only qualitative changes, a supercritical current increases the water depth upon entering shallow water, and is found to cause greater instability. The nonlinear consequence is that soliton fission can occur if a wave packet propagates into a shallower sea. For a subcritical current opposing the waves, Stokes waves can be unstable and soliton fission is possible in all depths as long as waves are not stopped.

2. Outline of derivation of the evolution equation

We introduce the small parameter ϵ to characterize the slope of the short waves and of the medium as follows:

$$ka = O(\epsilon), \quad \frac{1}{kh}\frac{\mathrm{d}h}{\mathrm{d}x} = \frac{1}{kU}\frac{\partial U}{\partial x} = \frac{1}{\omega U}\frac{\partial U}{\partial t} = O(\epsilon^2), \tag{2.1}$$

where ω, k and a are the characteristic frequency, wavenumber and wave amplitude of the short waves, and h and U are the still-water depth and current velocity respectively. The depth is only a function of x, and U is in the x-direction (see figure 1). It is further assumed that

$$kh = O(1), \tag{2.2}$$

$$U(gh)^{-\frac{1}{2}} \leqq O(1). \tag{2.3}$$

Thus the current can be strong. For convenience we shall say that $U = O(1)$ without formal normalization.

In the absence of waves and vorticity ($\Omega_z \leqq O(\epsilon^4)$), the current velocity U and the associated free-surface displacement ζ satisfy Airy's nonlinear equations for shallow water waves

$$\frac{\partial \zeta}{\partial t} + \frac{\partial}{\partial x}[U(\zeta+h)] = O(\epsilon^4), \tag{2.4}$$

$$\frac{\partial U}{\partial t} + U\frac{\partial U}{\partial x} + g\frac{\partial \zeta}{\partial x} = O(\epsilon^4), \tag{2.5}$$

$$P = \rho g(\zeta - z) + O(\epsilon^4). \tag{2.6}$$

Terms on the left of (2.4) and (2.5) are $O(\epsilon^2)$ because of the assumed time- and lengthscales. It can be shown that the local horizontal velocity of the current is independent of the vertical coordinate z with an error of $O(\epsilon^4)$. From the exact equation of continuity, the vertical current velocity is $O(\epsilon^2)$:

$$W = (z+h)\frac{\partial U}{\partial x} - \frac{\partial h}{\partial x}U + O(\epsilon^4). \tag{2.7}$$

To study the effect of currents on waves, we substitute

$$\boldsymbol{u}_{\text{total}} = (U+u, w), \quad \zeta_{\text{total}} = \zeta+\eta, \quad p_{\text{total}} = P+p \tag{2.8}$$

into the full Euler equations and the boundary conditions. By assumption, u, w, p and η are $O(\epsilon)$, and derivatives operating on them are of order unity. We then obtain from continuity and momentum conservation a combined equation for wave pressure p:

$$\nabla^2 p = -\rho\left\{2\left(\frac{\partial u}{\partial x}\right)^2 + 2\frac{\partial w}{\partial x}\frac{\partial u}{\partial z} + 4\frac{\partial u}{\partial x}\frac{\partial U}{\partial x}\right\} + O(\epsilon^4) \quad (-h < z < \zeta+\eta). \tag{2.9}$$

From the condition that there is no velocity normal to the sea bottom, we obtain

$$\frac{\partial p}{\partial z} = -\frac{\mathrm{d}h}{\mathrm{d}x}\frac{\partial p}{\partial x} + O(\epsilon^4), \quad z = -h(x). \tag{2.10}$$

The kinematic condition on the free surface can be expanded about $z = \zeta$, with the result

$$\frac{\partial \eta}{\partial t} + u\frac{\partial \zeta}{\partial x} + U\frac{\partial \eta}{\partial x} = -\eta\frac{\partial U}{\partial x} + w + \eta\frac{\partial w}{\partial z} - u\frac{\partial \eta}{\partial x} - \eta\frac{\partial \eta}{\partial x}\frac{\partial u}{\partial z} + \frac{\eta^2}{2}\frac{\partial^2 w}{\partial z^2} + O(\epsilon^4) \quad (z = \zeta) \tag{2.11}$$

The dynamic condition that $\mathrm{D}p/\mathrm{D}t = 0$ on $z = \zeta+\eta$ can be expanded similarly to yield

$$\begin{aligned}
&\frac{\partial p}{\partial t} + \eta\frac{\partial^2 p}{\partial t\,\partial z} + \frac{\eta^2}{2}\frac{\partial^3 p}{\partial t\,\partial z^2} + U\frac{\partial p}{\partial x} + U\eta\frac{\partial^2 p}{\partial z\,\partial x} \\
&\quad + U\frac{\eta^2}{2}\frac{\partial^3 p}{\partial z^2\,\partial x} + u\frac{\partial p}{\partial x} + \eta\frac{\partial p}{\partial x}\frac{\partial u}{\partial z} + u\eta\frac{\partial^2 p}{\partial x\,\partial z} \\
&\quad + w\frac{\partial p}{\partial z} + \eta\frac{\partial p}{\partial z}\frac{\partial w}{\partial z} + w\eta\frac{\partial^2 p}{\partial z^2} \\
&\quad + \rho g u\frac{\partial \zeta}{\partial x} + W\frac{\partial p}{\partial z} + \rho g\eta\frac{\partial U}{\partial x} - \rho g\left(w + \eta\frac{\partial w}{\partial z} + \frac{\eta^2}{2}\frac{\partial^2 w}{\partial z^2}\right) = O(\epsilon^4) \quad (z = \zeta).
\end{aligned} \tag{2.12}$$

Next we make explicit use of the slow coordinates

$$X = \epsilon^2 x, \quad T = \epsilon^2 t, \tag{2.13a}$$

so that $U = U(X, T)$ and $\zeta = \zeta(X, T)$, and introduce the moving coordinate

$$\xi = \epsilon\left(\int \frac{\mathrm{d}x}{C_g(X, T)} - t\right). \tag{2.13b}$$

We shall restrict our attention to waves that propagate in the positive x-direction. The following WKB expansions are then introduced:

$$\eta(x, t) = \sum_{n=1}^{\infty} \sum_{m=-n}^{n} \epsilon^n \eta_{nm} \mathrm{e}^{\mathrm{i}m\phi}, \tag{2.14a}$$

$$p(x, z, t) = \sum_{n=1}^{\infty} \sum_{m=-n}^{n} \epsilon^n P_{nm} \mathrm{e}^{\mathrm{i}m\phi}, \tag{2.14b}$$

where

$$\eta_{nm} = \eta_{nm}(X, T, \xi) = \eta^*_{n,-m}, \tag{2.15a}$$

$$P_{nm} = P_{nm}(X, T, z, \xi) = P^*_{n,-m}, \tag{2.15b}$$

$$k = \frac{\partial \phi(X, T)}{\partial X}, \quad \omega = -\frac{\partial \phi(X, T)}{\partial T} \tag{2.15c}$$

and $(\,)^*$ denotes the complex conjugate of $(\,)$.

Expansions for u and w are similar to (2.14b). The perturbation procedure is lengthy but straightforward, and is in principle, similar to that used by Chu & Mei (1970), Davey & Stewartson (1974) and Djordjevic & Redekopp (1978). Details are omitted, but may be found in Turpin (1981), with corrections by Benmoussa (1982). In particular, the first-order first-harmonic amplitude of wave pressure is

$$P_{11} = A \frac{\cosh k(z+h)}{\cosh kd}, \tag{2.16}$$

where

$$d = \zeta + h \tag{2.17}$$

denotes the mean water depth including the current set-up. The following dispersion relation holds:

$$\sigma^2 \equiv (\omega - Uk)^2 = gk \tanh kd, \tag{2.18}$$

the properties of which are well known (see e.g. Peregrine 1976). Let

$$C_p = \frac{\sigma}{k}, \tag{2.19}$$

$$C_g = U + \frac{1}{2}\frac{\sigma}{k}\left(1 + \frac{2kd}{\sinh 2kd}\right) \tag{2.20}$$

denote the phase and group velocities respectively, and set

$$\beta = \tanh kd \tag{2.21}$$

for brevity. Then A is governed by the following cubic Schrödinger equation:

$$\alpha_1 A + \frac{1}{C_g} A_T + A_X + i\alpha_2 A_{\xi\xi} + i\alpha_3 |A|^2 A = 0, \tag{2.22}$$

where the coefficients are

$$\alpha_1(X, T) = -\frac{1}{2\sigma C_g}\frac{\partial \sigma}{\partial T} + \frac{\sigma}{2C_g}\frac{\partial}{\partial X}\left(\frac{C_g}{\sigma}\right), \tag{2.23a}$$

$$\alpha_2(X, T) = \frac{1}{2\sigma C_g}\frac{(C_g - U)^2}{C_g^2}\left[1 - \frac{gd}{(C_g - U)^2}(1-\beta^2)(1-\beta kd)\right]$$

$$= -\frac{1}{2C_g^3}\frac{\partial^2 \omega}{\partial k^2} = -\frac{1}{2C_g^3}\frac{\partial^2 \sigma}{\partial k^2}, \tag{2.23b}$$

$$\alpha_3(X, T) = \frac{k^4}{4\rho^2\sigma^3\beta^2 C_g}\left\{9 - 10\beta^2 + 9\beta^4 - \frac{2\beta^2(C_g - U)^2}{gd - (C_g - U)^2}\right.$$

$$\left.\times\left[4\left(\frac{C_p}{C_g - U}\right)^2 + 4\left(\frac{C_p}{C_g - U}\right)(1-\beta^2) + \frac{gd}{(C_g - U)^2}(1-\beta^2)^2\right]\right\}. \tag{2.23c}$$

In the special case of vanishing current, (2.22) and (2.23) reduce to those of Djordjevic & Redekopp for variable depth. Indeed the formal effect of a strong current is simply to change h to d and ω to σ, with the associated changes in C_g and C_p. For constant depth the result of Davey & Stewartson (1974) is recovered.

The stipulation that the current is not affected by short waves holds as long as $h = h(\epsilon^2 x)$ and the length- and timescales of the current outside the wavepacket are $O(\epsilon^{-1})$ larger than those of the wave envelope for any current strength within the range $O \leqslant U(gh)^{-\frac{1}{2}} \leqslant O(1)$. Although our starting assumption was at the upper limit that $U(gh)^{-\frac{1}{2}} = O(1)$, the result was already seen to hold for the lower limit of $U = 0$. Consider an intermediate magnitude, say $U(gh)^{-\frac{1}{2}} = O(\epsilon)$. We can then allow zeroth harmonics u_{10}, η_{10} and p_{10} at the first order in the perturbation analysis. They are, however, found to depend only on X and T and not on the lengthscale of the wavepacket. Moreover, they are governed by the linearized version of (2.4) and (2.5) and initial and boundary conditions for upstream. Therefore the case of an $O(\epsilon)$ current is merely a special case of strong current. If, on the other hand, $h = h(\epsilon x)$, the current and wavepacket have comparable length-scales. We then expect the current to be affected by the short waves, since it is well known in constant depth that even a second-order $O(\epsilon^2)$ current is affected by wave modulation (Benney & Roskes 1969; Chu & Mei (1970; Davey & Stewartson 1974).

Once U and ζ are known from Airy's equations, A can be solved in principle for suitable initial and boundary conditions.

In practice the solution for transient Airy's equations is an involved task in itself; we shall therefore limit our subsequent discussion to a steady current.

For later purposes we introduce the following normalized variables:

$$\left.\begin{aligned}
(U', C_g', C_p') &= (U, C_g, C_p)(gh_1)^{-\frac{1}{2}}, \\
X' &= \frac{x}{h_1}\left(\frac{a}{h_1}\right)^2, \quad \xi' = \xi\left(\frac{g}{h_1}\right)^{\frac{1}{2}}\frac{a}{h_1}, \\
A' &= \frac{A}{\rho g a}, \quad k' = kh_1, \\
d' &= \frac{d}{h_1} = \frac{\zeta + h}{h_1}, \quad \sigma' = \left(\frac{g}{h_1}\right)^{\frac{1}{2}}\sigma, \\
\text{wave period } \tau &= \frac{2\pi}{\omega}\left(\frac{h_1}{g}\right)^{\frac{1}{2}},
\end{aligned}\right\} \tag{2.24}$$

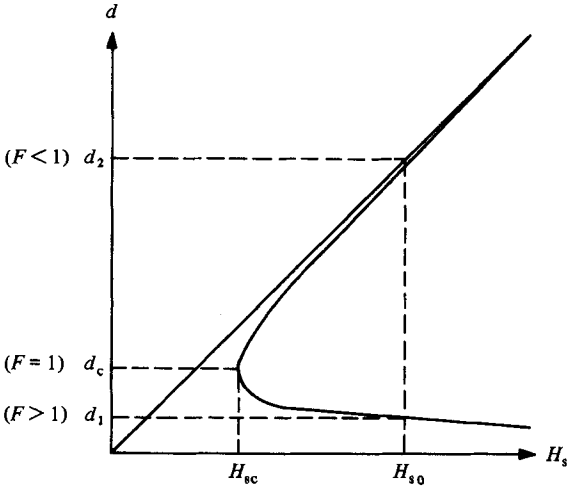

FIGURE 2. Specific-head diagram.

where a and h_1 represent respectively the wave amplitude and a reference depth. We shall henceforth omit the primes for brevity.

Equations (2.22) preserves its form after the normalization except that α_1', α_2' and α_3' (with primes omitted) are obtained from (2.23a, b, c) by simply omitting g and ρ.

With the help of the transformation (Djordjevic & Redekopp 1978)

$$\overline{X} = \int_0^X \alpha_2(u)\,\mathrm{d}u, \tag{2.25}$$

$$A = B\exp\left(-\int_0^X \alpha_1(u)\,\mathrm{d}u\right) = sB, \tag{2.26}$$

(2.22) can be put in the canonical form

$$-\mathrm{i}B_{\overline{X}} + B_{\xi\xi} + K|B|^2B = 0, \tag{2.27}$$

where

$$K = \frac{\alpha_3}{\alpha_2}s^2, \tag{2.28a}$$

$$s = \left[\left(\frac{C_g}{\sigma}\right)_1 \Big/ \left(\frac{C_g}{\sigma}\right)\right]^{\frac{1}{2}} = \exp\left(-\int_0^X \alpha_1(u)\,\mathrm{d}u\right), \tag{2.28b}$$

with the subscript 1 denoting values at $X = \overline{X} = 0$. The quantity s depends only on X or $\overline{X}$ and is known to be the *shoaling factor* of infinitesimal waves.

3. Properties of a stationary current on a slowly varying depth

For a stationary current with $\partial/\partial T = 0$, existing knowledge in open-channel hydraulics can be applied. Some of the salient features are summarized below. After integrating Airy's equation with respect to X, we obtain

$$(\zeta + h)\,U = U_1 h_1, \tag{3.1}$$

$$\tfrac{1}{2}U^2 + g\zeta = \tfrac{1}{2}U_1^2, \tag{3.2}$$

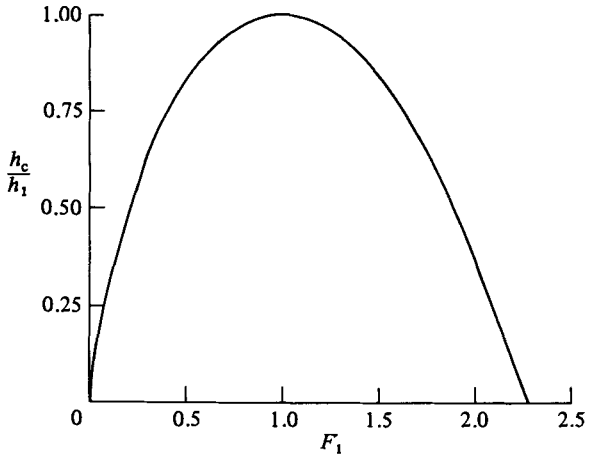

FIGURE 3. Critical depth.

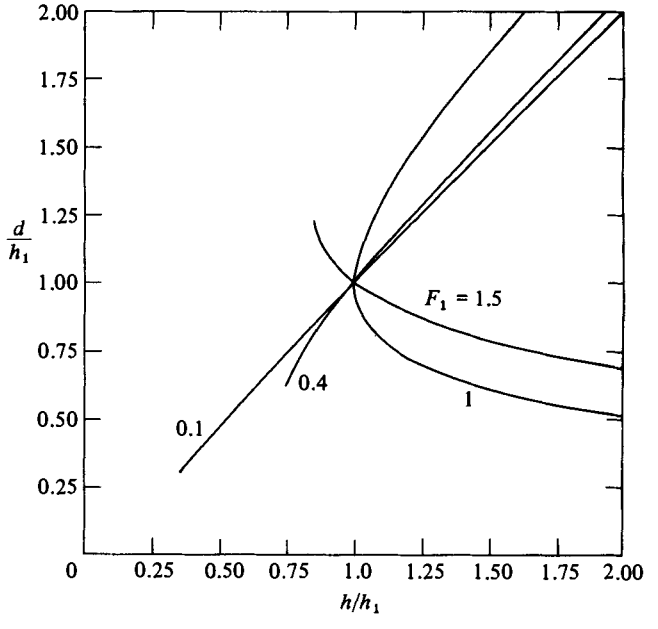

FIGURE 4. Set-up due to the current.

where U_1 and h_1 refer to the constant values at $X \to -\infty$. Defining the *specific head* by

$$H_s = \frac{U^2}{2g} + (\zeta + h) \equiv \frac{U^2}{2g} + d, \tag{3.3}$$

we can eliminate U to get

$$H_s = \frac{(U_1 h_1)^2}{2gd^2} + d, \tag{3.4}$$

which is plotted in figure 2. The smallest H_s occurs at

$$d_c = (U_1 h_1)^{\frac{2}{3}} g^{-\frac{1}{3}}, \tag{3.5}$$

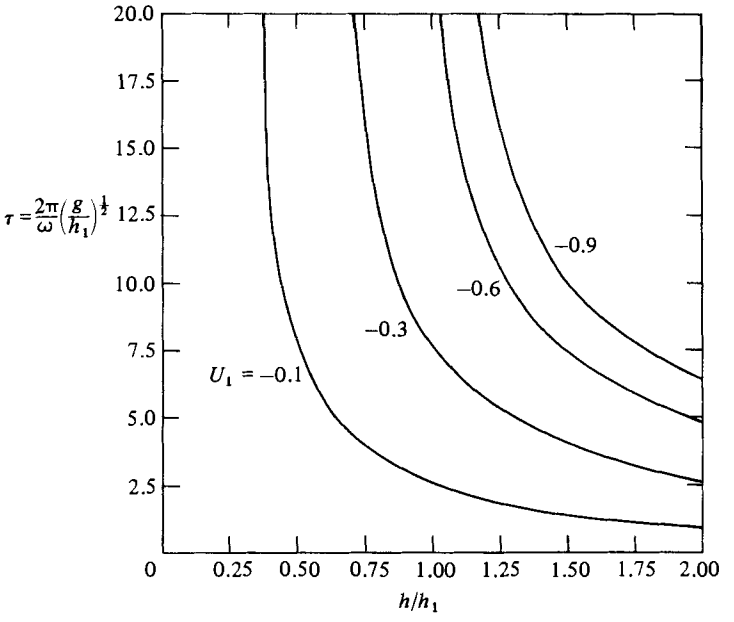

FIGURE 5. Stopping periods for negative currents.

below which there can be no stationary current. The corresponding specific head, still-water depth and Froude number are respectively

$$(H_s)_c = \tfrac{3}{2}d_c = \tfrac{3}{2}(U_1 h_1)^{\frac{2}{3}} g^{-\frac{1}{3}}, \quad h_c = \tfrac{2}{3}d_c - \frac{U_1^2}{2g} = H_{sc} - \frac{U_1^2}{2g}, \quad F_c = U_c(gd_c)^{-\frac{1}{2}} = 1. \tag{3.6a,b,c}$$

These values define the *critical flow*. Figure 3 shows the variation of h_c/h_1 *vs.* the Froude number $F_1 = U_1(gh_1)^{-\frac{1}{2}}$. Thus a steady current is possible if $h > h_1$ everywhere or $F_1 > 3^{\frac{3}{2}}$. From (3.1) and (3.2) a cubic equation can be derived for $d = \zeta + h$:

$$\left(\frac{d}{h_1}\right)^3 - \left(\frac{h}{h_1} + \frac{1}{2}F_1^2\right)\left(\frac{d}{h_1}\right)^2 + \tfrac{1}{2}F_1^2 = 0. \tag{3.7}$$

Typical solutions are plotted in figure 4, which shows that d/h_1 decreases or increases as h/h_1 increases, for $F_1 > 1$ (supercritical flow) or $F_1 < 1$ (subcritical flow) respectively. For the critical flow $F_1 = 1$; two total depths are possible for the same h/h_1.

4. Analytical aspects of waves

4.1. *Dispersion relation*

As is well known (see e.g. Peregrine 1976), a positive current (in the positive x-direction along which the waves are assumed to propagate) tends to lengthen the waves while a negative current shortens them. Corresponding to a given depth and negative current there is a certain period at which a sinusoidal wavetrain cannot propagate. For later reference the stopping periods are plotted in figure 5 against h/h_1 for various values of F_1.

4.2. *Shoaling of an infinite train of Stokes waves*

If the initial and boundary conditions are such that a Stokes wavetrain is unmodulated on the physical length- and timescales $O(k\epsilon)^{-1}$ and $O(\omega\epsilon)^{-1}$ respectively, then A depends on X only, but not on ξ. In view of (2.26), B is a function of $\bar{X}$ only, and (2.27) may be easily integrated:

$$\frac{B(\bar{X})}{B(0)} = \exp\left(-\mathrm{i}\,B^2(0)\int_0^{\bar{X}}\frac{\alpha_3}{\alpha_2}s^2\mathrm{d}v\right), \tag{4.1}$$

where $B(0)$ can be taken to be real. Thus nonlinearity affects the phase of $B(\bar{X})$ only. Combining (2.26) with (4.1), we obtain

$$A = sB(0)\exp\left(-\mathrm{i}\,B^2(0)\int_0^{\bar{X}}\frac{\alpha_3}{\alpha_2}s^2\,\mathrm{d}v\right), \tag{4.2}$$

which is the result for Stokes waves on a variable medium. Note that

$$\frac{A(X)}{A(0)} = s = \left[\left(\frac{C_g}{\sigma}\right)_1\Big/\left(\frac{C_g}{\sigma}\right)\right]^{\frac{1}{2}}, \tag{4.3}$$

where $A(0) = B(0)$. Thus the first-order first-harmonic amplitude of a Stokes wave varies with x according to the shoaling law of infinitesimal waves.

4.3. *Sideband instability*

Existing theories on the sideband instability are all for constant depth, so that the coefficients of the Schrödinger equation are constants. Here the coefficient $(\alpha_3/\alpha_2)\,s^2$ depends only on $\bar{X}$, and the *spatial* instability can still be examined in the standard manner.

Letting
$$B(X,\xi) = b(\bar{X},\xi)\,\mathrm{e}^{\mathrm{i}f(\bar{X},\xi)}, \tag{4.4}$$

where b and f are both real, then

$$\frac{\partial b^2}{\partial\bar{X}} - \frac{\partial}{\partial\xi}(b^2W) = 0, \quad \frac{\partial W}{\partial\bar{X}} + \frac{\partial}{\partial\xi}\left(\frac{b_{\xi\xi}}{b} - W^2 + Kb^2\right) = 0, \tag{4.5a, b}$$

with
$$W = f_\xi.$$

Linearizing with respect to the Stokes wave $b = b_0$ and $W = 0$, i.e.

$$b = b_0 + b', \quad W = w', \tag{4.6}$$

and assuming a slowly varying perturbation in the form of a propagating wave:

$$\begin{bmatrix} b' \\ W' \end{bmatrix} = \begin{bmatrix} \hat{b} \\ \hat{W} \end{bmatrix}\exp\mathrm{i}\,(\phi(\bar{X}) - \Omega\xi), \tag{4.7}$$

we find the eigenvalue condition

$$\frac{\mathrm{d}\phi}{\mathrm{d}\bar{X}} = \Omega b_0\left(\frac{\Omega^2}{2b_0^2} - K\right)^{\frac{1}{2}} \tag{4.8}$$

If $K > 0$, $\mathrm{d}\phi/\mathrm{d}x$ can be imaginary, and the sideband disturbance grows spatially in $\bar{X}$, and hence is unstable. K will be referred to as the instability parameter.

Since the sign dependence of α_3 on kd is the same as in the case of constant depth (cf. Davey & Stewartson 1974) and since $\alpha_2 > 0$ always, the shoaling Stokes wavetrain is unstable if $kd > 1.363$, where kd now depends on the current.

5. Numerical procedure for solving the evolution equation

After the current and its mean sea level were calculated, a semi-implicit finite-difference scheme of Crank–Nicolison type was applied to (2.22) directly to solve for A. Only wavepackets were considered so that $|A| \downarrow 0$ as $|\xi| \uparrow \infty$. The boundary conditions in the computational schemes are that $A = 0$ at $\xi = \pm \xi_0$, where ξ_0 was chosen large enough (and different in different cases) so that further increase in ξ did not change the result. The conservation law

$$\frac{C_g}{\sigma} \int_{-\infty}^{\infty} |A|^2 \, d\xi = \text{const.} \tag{5.1}$$

holds and was used to check the global accuracy. Satisfactory confirmation was first obtained for a permanent soliton on a constant depth.

The botton geometry examined was a smooth slope connecting two different but constant depths: $h = 1$, $X < 0$; $h = 1 + dh$, $X > 0$. The transition was specified to be

$$h = 1 + \tfrac{1}{2} dh \, (1 - \cos \pi X) \quad (0 \leqslant X \leqslant 1), \tag{5.2}$$

and the parameter dh was varied. The initial envelope was taken to be

$$A(0, \xi) = \operatorname{sech}\left[\left(\frac{|\alpha_3(0)|}{2\alpha_2(0)}\right)^{\frac{1}{2}} \xi\right] = \operatorname{sech}\left[(\tfrac{1}{2}|K(0)|^{\frac{1}{2}} \xi\right]. \tag{5.3}$$

When $\alpha_3(0) > 0$, this represents a soliton, which propagates over constant depth ($h = 1$) without any shape variation. The required spatial domain on the ξ-axis depended on $(\alpha_3(0)|/2\alpha_2(0))^{-\frac{1}{2}}$ and was made sufficiently large throughout the integration.

We first discuss the results of pure depth variation without current. At the start of the slope $X = 0$, the Froude number F_1 at $X \to -\infty$ and the normalized short wave period τ were prescribed.

6. Evolution of a wave packet on a varying depth

In figure 6 we plot the inverse of the shoaling coefficient $(C_g/\sigma)/(C_g/\sigma)_1 = s^2$, the dispersion relation and the instability parameter $K = s^2 \alpha_3/\alpha_2$ as functions of local depth h/h_1, with the dimensionless wave period τ as the parameter. A shorter period implies a larger kd, s and K. For all frequencies, the zeros of K occur at $kd = 1.363$; the corresponding h/h_1 increases with shorter period.

We experimented with various cases where an initial wavepacket travelled in the direction of increasing or decreasing K, in regions where K was either positive, or negative, or changed sign.

(i) $K > 0$ for all X. In figure 7 computed results are shown for $\tau = 5$ for $dh = 0.3$ (i.e. $h_1 = 1$, $h_2 = 1.3$). At the beginning and the end of the slope we have

$$(kd)_1 = (kh)_1 = 1.69, \quad (K)_1 = 1.4 \quad (X = 0),$$

$$(kd)_2 = (kh)_2 = 2.11, \quad (K)_2 = 2.18 \quad (X = 1).$$

Thus the initial envelope, which was a soliton, propagated in the direction of increasing instability ($K \uparrow$). At $X = 1$ the envelope was no longer a soliton; and has two side groups separated by nodes. The qualitative evolution picture in figure 7 (a) is similar to the case of two bound solitons, where there is a single recurrence period after which the profile repeats itself. However, in this case, recurrence is accompanied

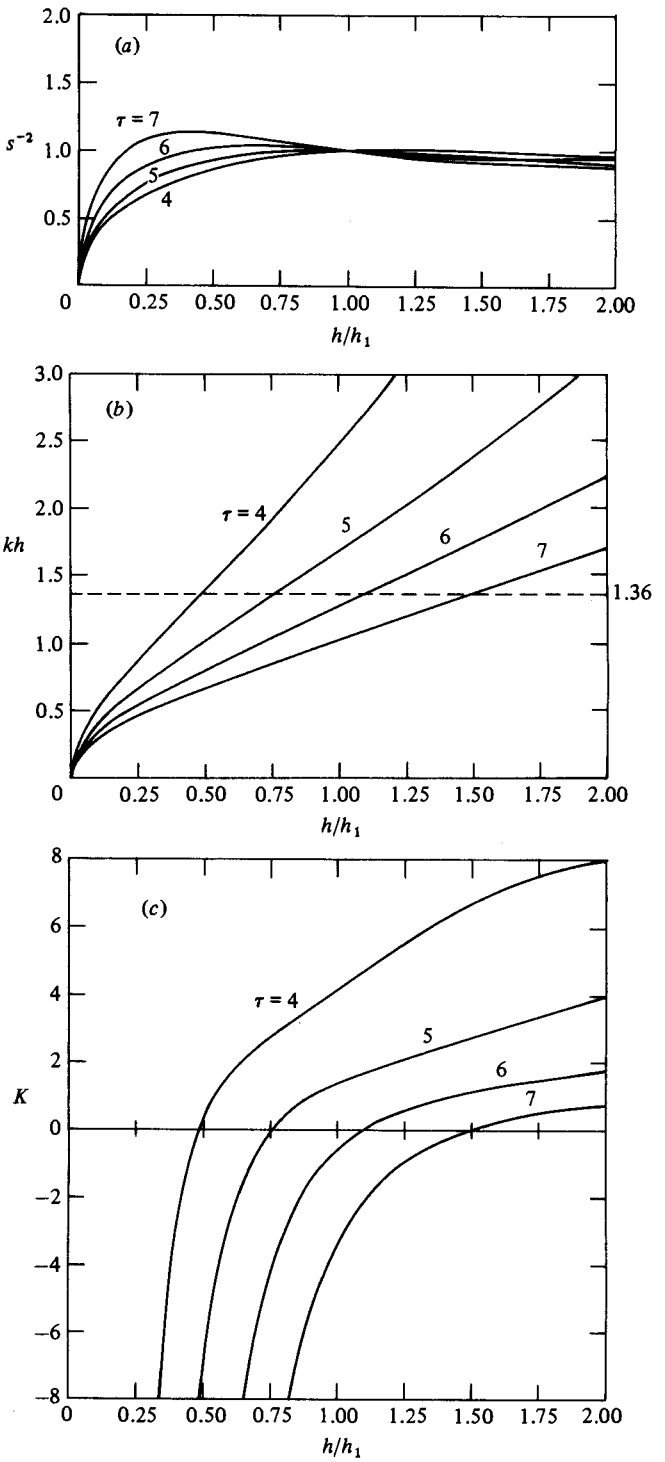

FIGURE 6. (*a*) Inverse of the shoaling coefficient s^{-2}; (*b*) wavenumber kh; (*c*) instability parameter K (no current).

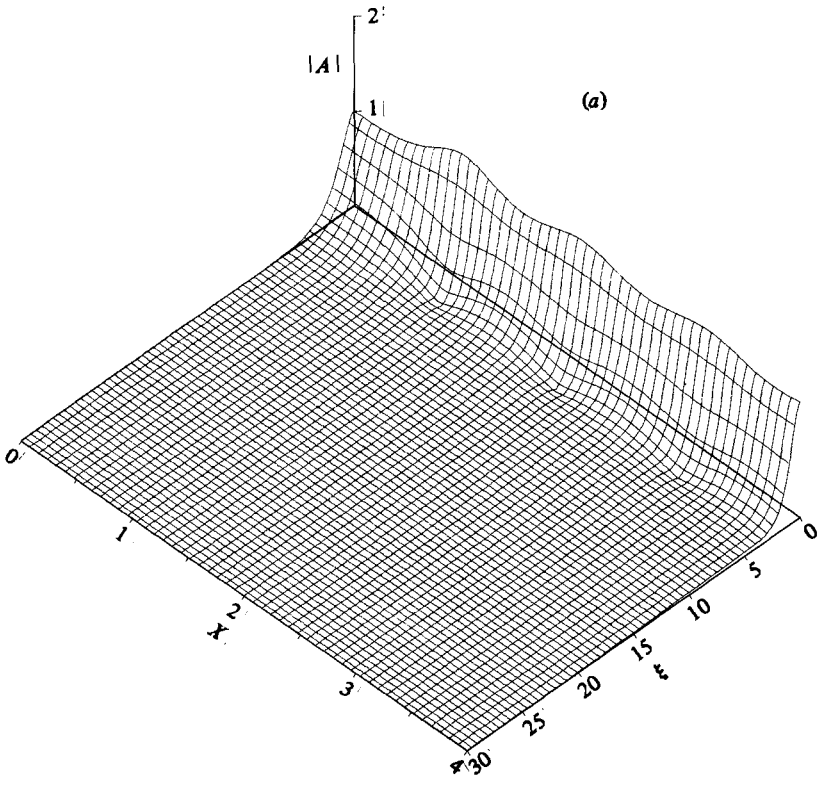

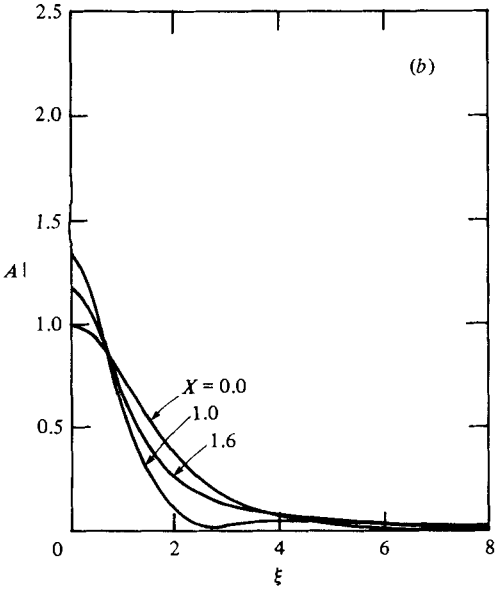

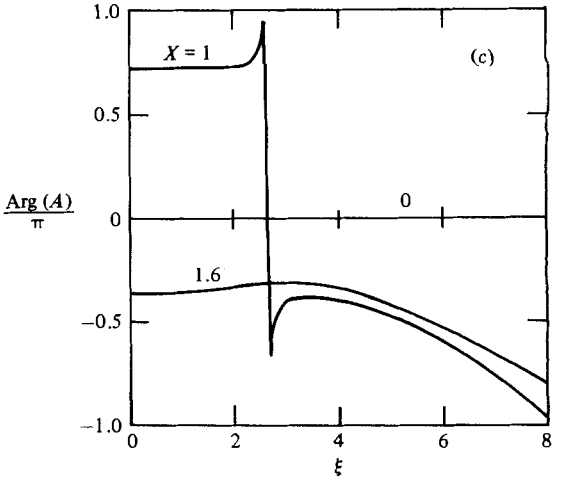

FIGURE 7. (*a*) 3-dimensional plot of the wave amplitude $|A(X, \xi)|$; (*b*) wave amplitude $|A(X, \xi)|$ and (*c*) phase Arg $(A(X, \xi))$ for $X = 0, 1, 1.6$; $F_1 = 0$, $\tau = 5$, $dh = +0.3$, $K_1 = 1.4$, $(kh)_1 = 1.69$, $K_2 = 2.18$, $(kh)_2 = 2.11$, $m = 1.5$, $\Delta = -26.6\,\%$, global energy error $= 2.5\,\%$.

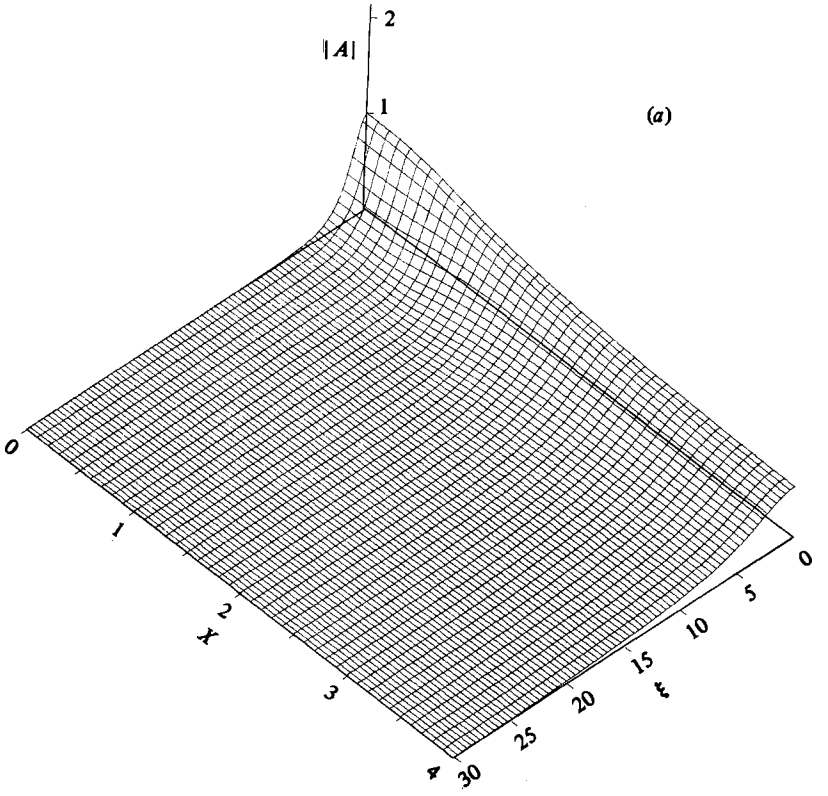

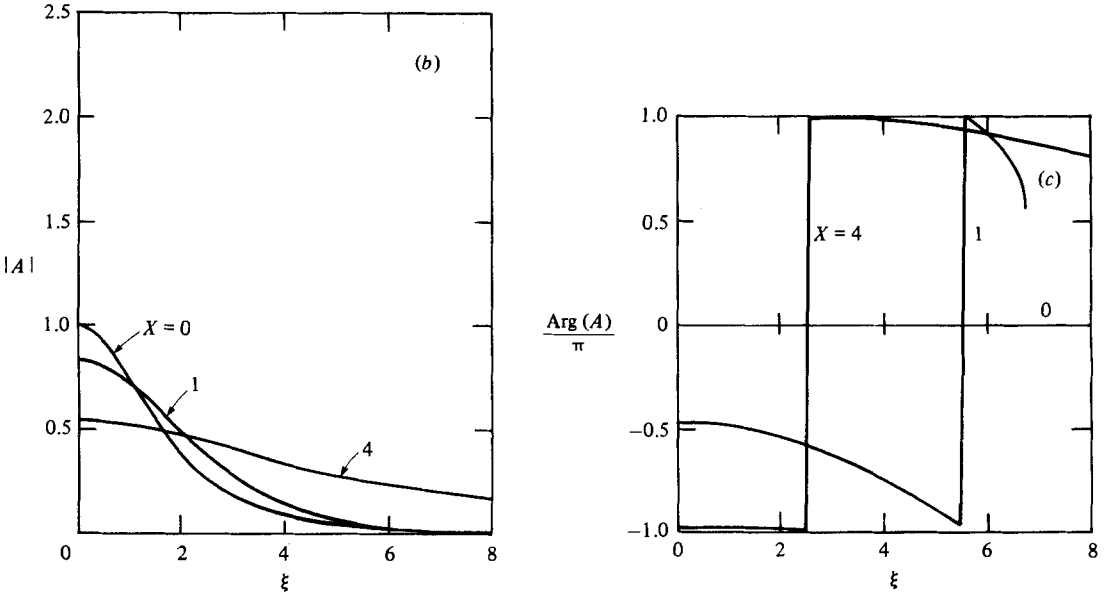

FIGURE 8. (*a*) 3-dimensional plot of the wave amplitude $|A(X, \xi)|$; (*b*) wave amplitude $|A(X, \xi)|$ and (*c*) phase Arg $(A(X, \xi))$ for $X = 0, 1, 4$; $F_1 = 0, \tau = 5, dh = -0.15, K_1 = 1.4, (kh)_1 = 1.69, K_2 = 0.72, (kh)_2 = 1.49, m = 1.3, \Delta = 10.8\,\%$, global energy error $= 0.1\,\%$.

by a slow decay of the maximum amplitude and a slight spreading towards large ξ, signalling radiation. Note in particular that the envelope at the start of the shelf ($X = 1$) already has two nodes and is quite different from a sech profile:

$$A = \bar{A} \operatorname{sech} \frac{\xi}{\lambda}. \tag{6.1}$$

Note also from figure 7(*c*) the sharp jump of phase by π across the envelope node, implying a peak of wave frequency or wavenumber. Because of the limited range of x computed, one cannot determine accurately the ultimate number of solitons on the shelf. For reference we note that for an initial envelope of the form (6.1), the asymptotic state consists of N solitons plus decaying oscillations, where N is the largest integer less than

$$m = \left(\frac{\alpha_3}{2\alpha_2}\right)^{\frac{1}{2}} \frac{\mathscr{A}}{\pi} + \frac{1}{2}, \tag{6.2}$$

where $\mathscr{A} = \pi \bar{A} \lambda$ is the total area of the initial envelope and α_3/α_2 is the initial instability parameter on the constant depth (Satsuma & Yajima, 1975). If $(\alpha_3/2\alpha_2)^{\frac{1}{2}} \mathscr{A}/\pi = N =$ integer, there are precisely N bound solitons. From further numerical experiments by Yue (1980) and ourselves, we know that, if $1 < m < 1.5$, there is a dispersive decay but no quasirecurrence. If $1.5 < m < 2.5$, recurrences typical of two bound solitons appear in addition; however only one soliton survives at the end if $1.5 < m \leqslant 2$, and two if $2 < m < 2.5$. For two initial envelopes of the same area and height, the evolution toward the final state can be quite different quantitatively if their shapes and phase distributions are different. The effect of phase has been examined by Benmoussa (1983), but no new qualitative features have been found.

By calculating numerically the area

$$\mathscr{A} = \int_{-\infty}^{\infty} |A| \, \mathrm{d}\xi \tag{6.3}$$

at the station $X = 1$, we may use (6.2) as a rough guide for the asymptotic state. For figure 7, $m = 1.5$, so that there should be only one soliton at $X \to \infty$. The fact that we see both recurrence and radiation is due to the initial departure from (6.1).

Keeping all the parameters fixed except dh, several numerical experiments showed that the position of the first envelope node, the internodal distance and the maximum amplitude were strongly dependent on the magnitude of dh. The larger the depth variation, the shorter is the distance of recurrence and the larger is the maximum amplitude.

Figure 8 shows an example where the envelope propagated toward decreasing depth ($K\downarrow$) although $K > 0$ (unstable) throughout. The envelope tended to flatten, but the heuristic estimation according to (6.2) and (6.3) indicates that it evolved into one soliton since $m = 1.3$. This has been further confirmed by comparing with the calculated evolution of another envelope which began at $X = 1$ with the same area and height but the form of (6.1). The two envelopes are nearly the same at $X = 4$. Therefore a soliton packet propagating into shallower water may achieve on the shelf a new balance between dispersion and nonlinearity although there is no fission. If the shallow water depth is such that K_2 tends to zero (for $\tau = 5$ this happens if $h/h_1 \to 0.75$ – see figure 6*c*) then the initial soliton envelope will just flatten steadily.

(ii) $K < 0$ for all X. No soliton can exist in this case, and the initial packet flattens whether the depth increases or decreases in the direction of propagation. Plots are omitted.

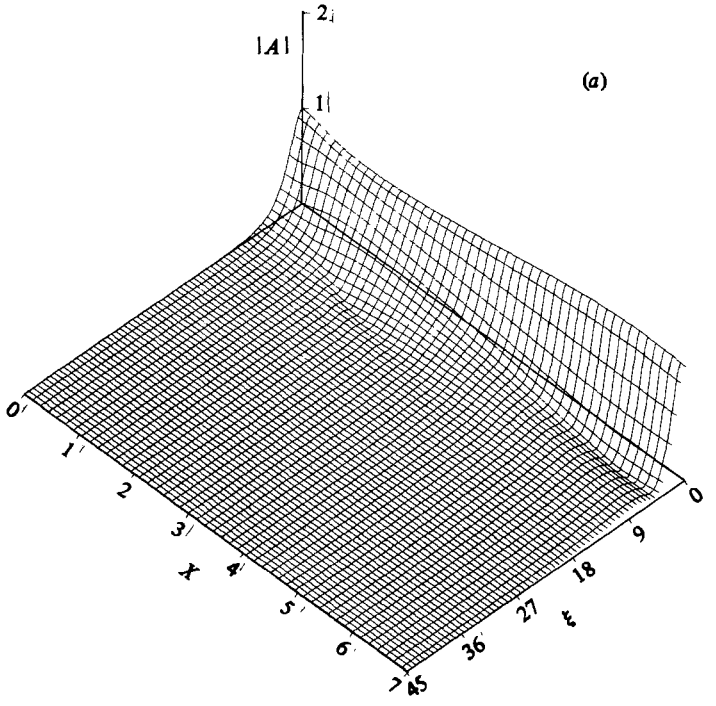

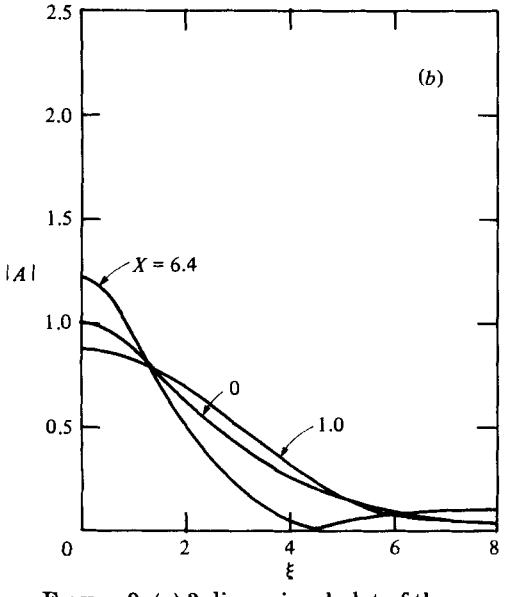

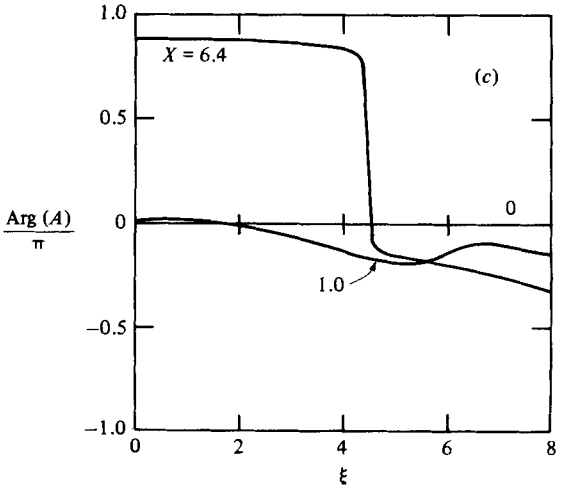

FIGURE 9. (*a*) 3-dimensional plot of the wave amplitude $|A(X, \xi)|$; (*b*) wave amplitude $|A(X, \xi)|$ and (*c*) phase Arg $(A(X, \xi))$ for $X = 0$, 1, 6.4; $F_1 = 0$, $\tau = 6$, $dh = +0.3$, $K_1 = -0.54$, $(kh)_1 = 1.28$, $K_2 = 0.73$, $(kh)_2 = 1.56$, $m = 1.7$, global energy error = 0.05 %.

(iii) K changes sign. Figure 9 shows the case of K increasing from -0.54 to 0.73 (kd from 1.28 to 1.56). The initial packet was not a soliton at $X = 0$, but soliton emission is clear in the deeper water ($m = 1.7$). If K decreases from positive to negative values, an initial soliton flattens and is not plotted here.

The emission of new solitons from a single soliton travelling into deeper water was first predicted by Djordjevic & Redekopp. Their estimation was based on (6.2) with an additional hypothesis on the envelope profile at $X = 1$. In terms of B defined by (2.26) and (2.27) they assumed that the initial soliton

$$B = B_0 \operatorname{sech} \nu\xi, \tag{6.4}$$

with

$$\nu = B_0(\tfrac{1}{2}K)_0^{\frac{1}{2}}, \tag{6.5}$$

preserved its form even after crossing the slope to $X = 1$. This of course implies that the wavepacket evolves in the same way as an infinite wavetrain, i.e. that the dependence on ξ is negligible. This assumption is not supported by the numerical results here as indicated in figures 7(*b*), 8(*b*) and 9(*b*) by the changes in shape and in dimensions of A from $X = 0$ to $X = 1$, despite the fact that the shoaling factor changed very little from $X = 0$ to $X = 1$. Since the estimation of the number of solitons emitted asymptotically depends on the area $\mathscr{A}$ of the envelope at $X = 1$, we compared this area calculated from our numerical result with that implied by Djordjevic & Redekopp:

$$\mathscr{A}_s = \pi\left[\left(\frac{2\alpha_2 C_g}{\alpha_3 \sigma}\right)_1 \Big/ \left(\frac{C_g}{\sigma}\right)_2\right]^{\frac{1}{2}}.$$

The ratio $\Delta = 1 - \mathscr{A}_s/\mathscr{A}$ is then a measure of discrepancy. Our numerical experiments showed that $\Delta \lessgtr 0$ when $dh \gtrless 0$ in general, and $\Delta = -26.6\,\%$ for figure 7, $\Delta = +10.8\,\%$ for figure 8. These discrepancies are sufficiently large to affect the number of soliton emission; hence the heuristic assumption of Djordjevic & Redekopp is not always reliable.

7. Effects of a steady current on changing depth on the evolution of a wavepacket

The important parameters kd, K and s now depend on $F_1 = U_1(gh_1)^{-\frac{1}{2}}$, i.e. the Froude number at $X \to -\infty$.

7.1. *Positive subcritical current* ($F_1 = 0.5$)

Figure 10 gives for various wave periods τ the inverse of the shoaling coefficient, the dispersion relation, and the instability parameter K, as functions of local depth of the still water. All results are given for h greater than the critical depth h_c. For the case shown, $F_1 = 0.5$; the critical depth is $h_c/h_1 = 0.38$, as can be read from figure 3. Comparing with the case of zero current, we first note the reduction of kd for the same h/h_1, implying the lengthening of waves by the positive current. As h increases, s now increases, since U decreases and C_g decreases also in greater depth. The lengthening of waves also shifts the curves of the instability parameter towards deeper water. Thus wave periods must be smaller in order for K to be positive at a given h/h_1. For the same topography as in the case without current (cf. figure 7, we note from figure 10(*c*) that $K < 0$ for $0 < h < 1.3$ if the same period $\tau = 5$ is assumed, and no solitons can exist with this current. However, for lower periods this positive subcritical current gives results qualitatively similar to those without current: soliton

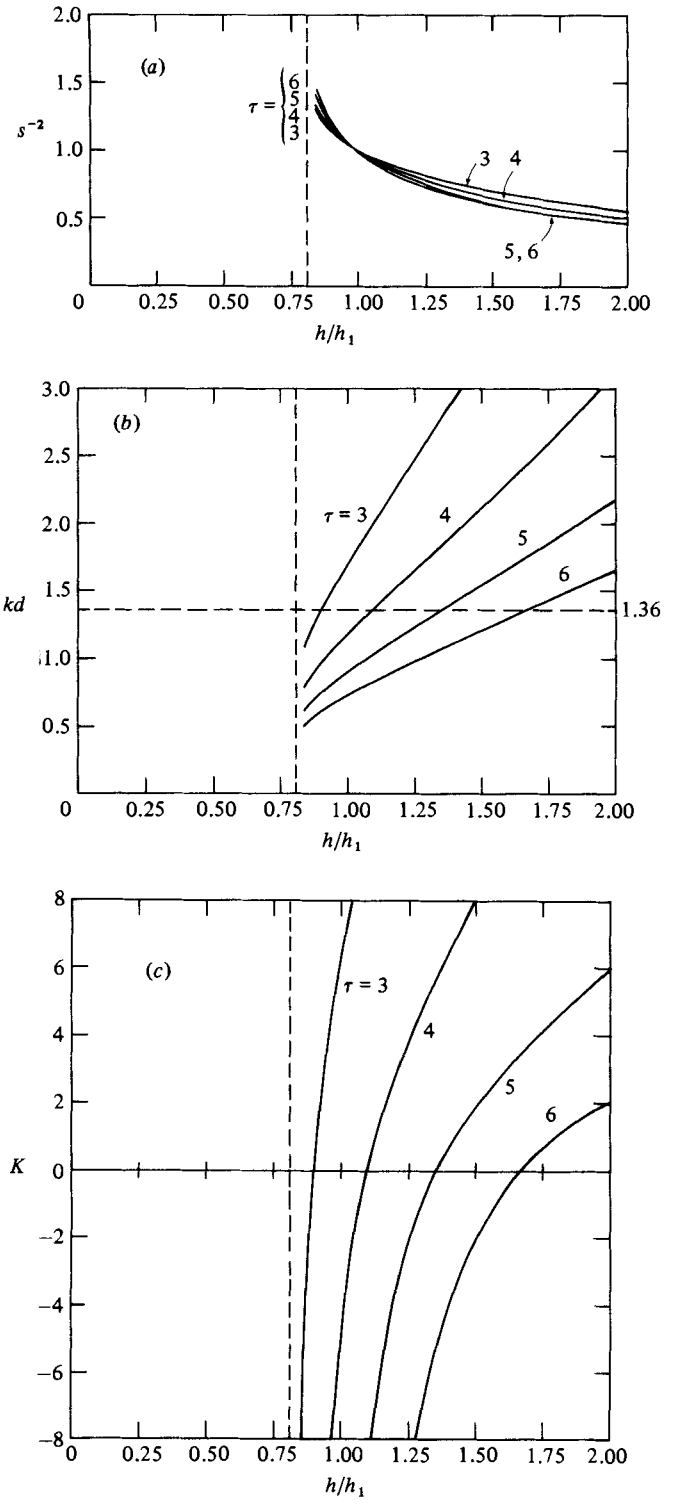

FIGURE 10. (*a*) Inverse of the shoaling coefficient s^{-2}; (*b*) wavenumber kd; (*c*) instability parameters K, for a subcritical current $F_1 = 0.5$.

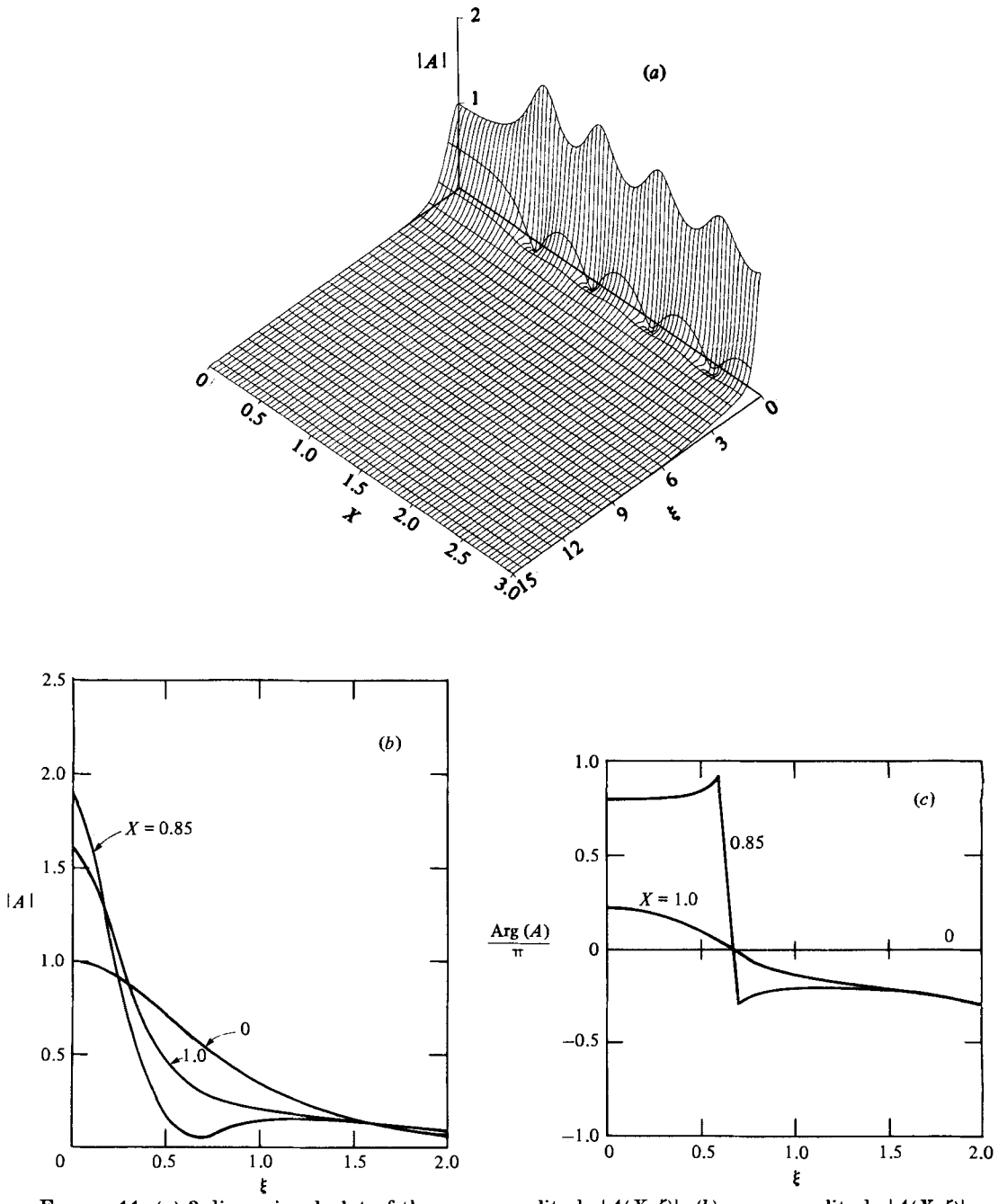

FIGURE 11. (*a*) 3-dimensional plot of the wave amplitude $|A(X,\xi)|$; (*b*) wave amplitude $|A(X,\xi)|$ and (*c*) phase Arg $(A(X,\xi))$ for $X = 0, 0.85, 1$; $F_1 = 0.5$, $\tau = 3$, $dh = +0.3$, $K_1 = 6.0$, $(kd)_1 = 1.68$, $K_2 = 15.6$, $(kd)_2 = 2.62$, $m = 1.9$, $\Delta = -15.2\,\%$, global energy error $= 5\,\%$.

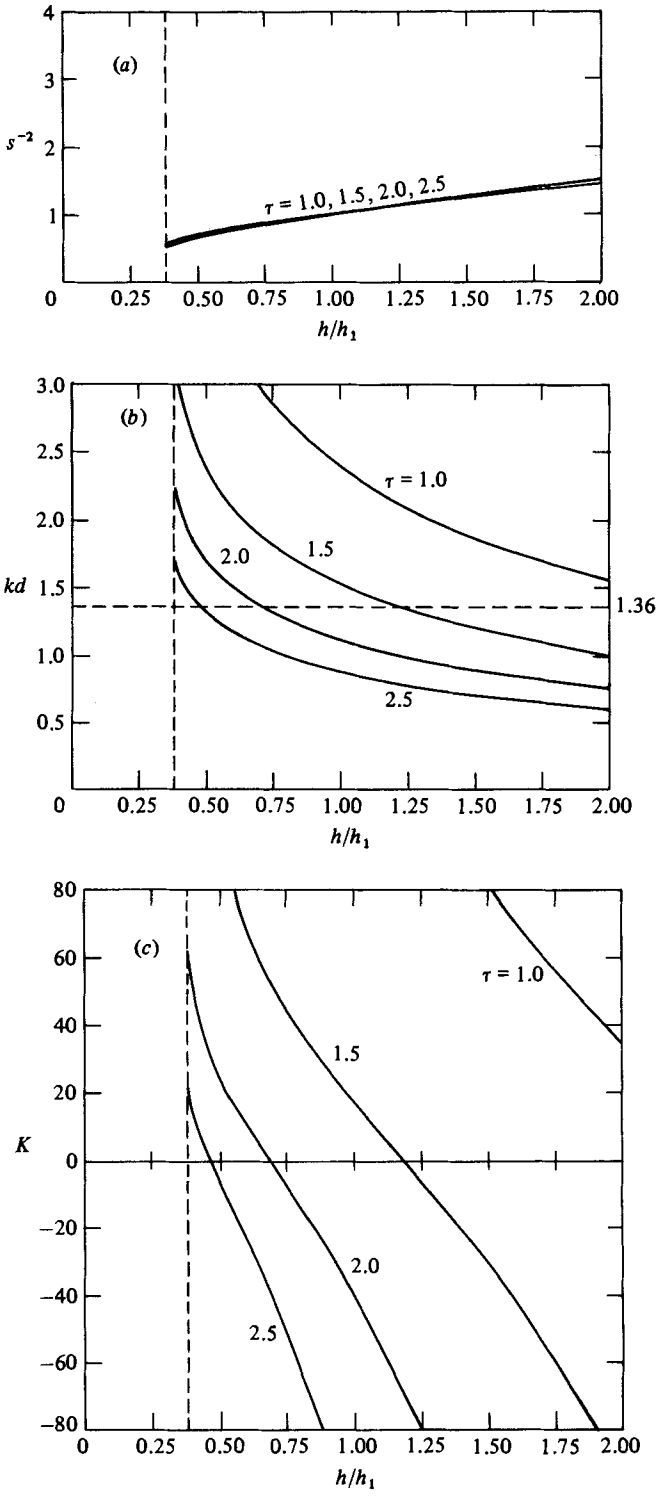

FIGURE 12. (*a*) Inverse of the shoaling coefficient s^{-2}; (*b*) wavenumber kd; (*c*) instability parameter K, for a supercritical current $F_1 = 2$.

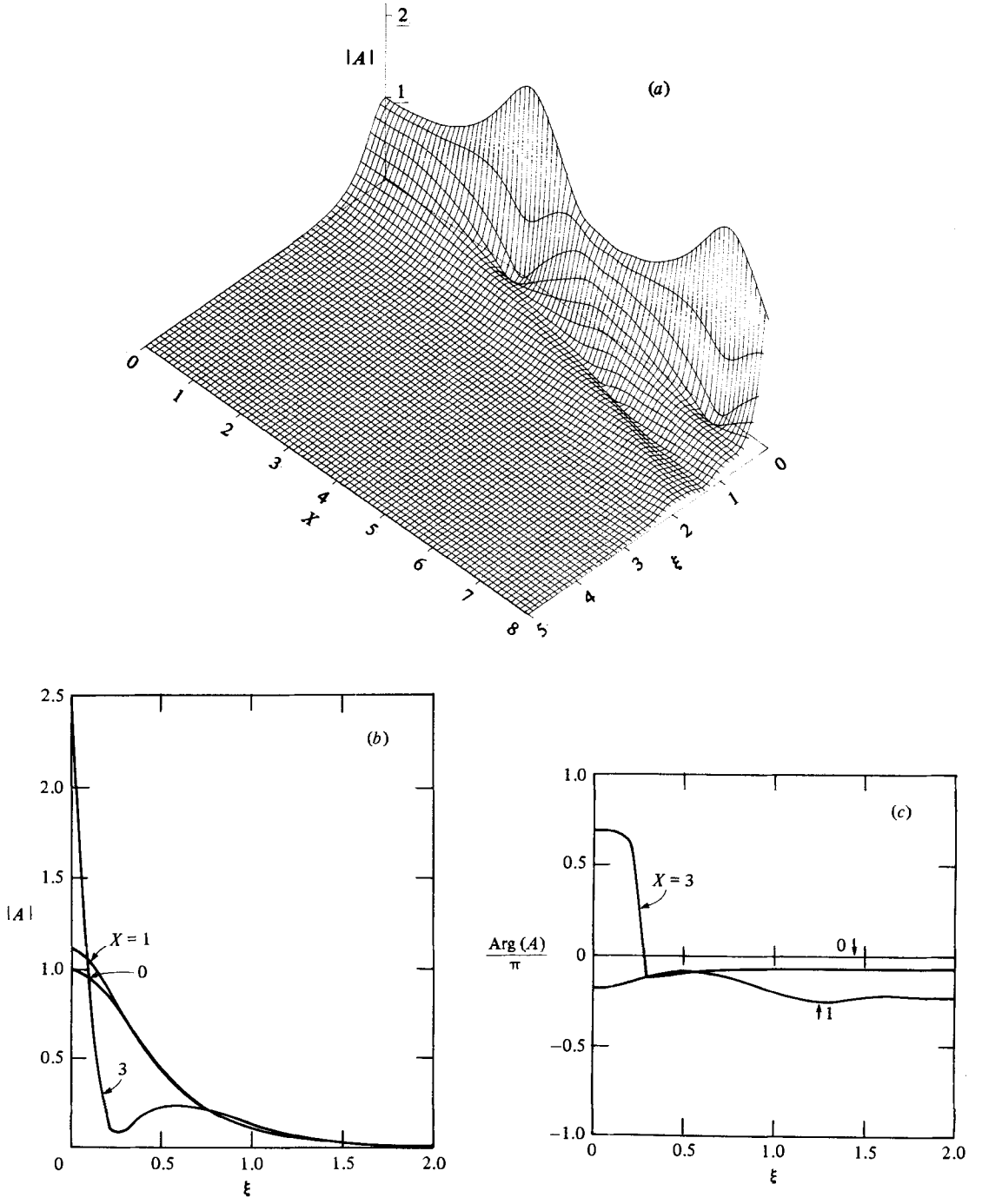

FIGURE 13. (*a*) 3-dimensional plot of the wave amplitude $|A(X,\xi)|$; (*b*) amplitude $|A(X,\xi)|$ and (*c*) phase Arg $(A(X,\xi))$ for $X = 0, 1, 3$; $F_1 = 2, \tau = 1.5, dh = -0.3, K_1 = 17.9, (kd)_1 = 1.51, K_2 = 48.1$, $(kd)_2 = 1.86$, $m = 2.1$, $\Delta = -0.9\,\%$, global energy error $= 0.2\,\%$.

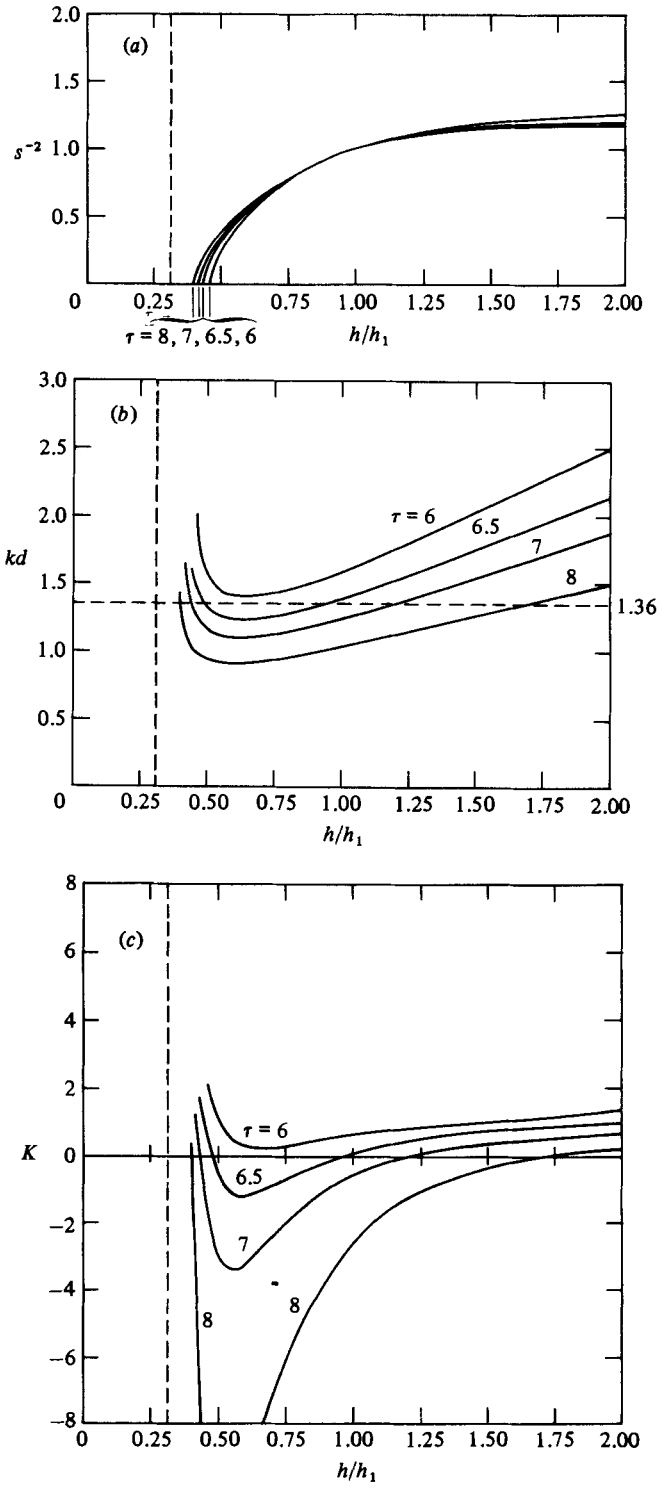

FIGURE 14. (*a*) Inverse of the shoaling coefficient s^{-2}; (*b*) wavenumber kd; (*c*) instability parameter K, for a negative current $F_1 = -0.1$.

emission is possible if the depth and the instability parameter increase in the direction of propagation. Figure 11 gives such an example for $\tau = 3$ and $dh = 0.3$. For this case $m = 1.9$, so that asymptotically only one soliton evolves. Djordjevic & Redekopp's assumption about shape conservation of the initial soliton along the slope can be extended without modification to the case with current, and would give $m_s = 2.1$, i.e. two solitons instead of one. It should be noted that this difference is important only asymptotically for large X; for a limited X the physical pictures are largely the same.

7.2. *Positive supercritical current*

In contrast with the previous cases, a positive supercritical current gives rise to smaller kd or longer waves as h/h_1 increases. The shoaling factor s also decreases from shallow to deep water. More important, the instability parameter K decreases with increasing h/h_1 (see figure 12). Thus Stokes waves are unstable in shallow water but stable in deep water! Figure 13 shows a case where the depth decreases from 1 to 0.7, but K is positive everywhere and increasing. The wave envelope envolves into two solitons ($m = 2.1$) plus some oscillation, which radiates for large X.

7.3. *Negative subcritical current*

We have selected a weak opposing current $F_1 = 0.1$ so that for the range of period computed the stopping depths implied by figure 5 were just slightly higher than the critical depth for the existence of the steady current. The left ends of all curves in Figure 14 correspond to the stopping depths at which $C_g = 0$. Most noteworthy is the fact that kd and K have a minimum around $h/h_1 = 0.6$ near the stopping depth; this is because the local wavenumber is large. Moreover, for sufficiently short waves ($\tau < 6.1$ here) $kd > 1.363$ and $K > 0$ for all h/h_1 greater than the stopping depth. Thus all Stokes waves are unstable! The envelope for $dh = 0.3$, $\tau = 6$, where kd increases from 1.58 to 1.83, again show near-recurrence. The figure is, however, omitted.

If the negative current is supercritical, no waves can exist. We omit all results for waves travelling into a region of decreasing instability. Suffice it to say that an initial soliton always flattens.

8. Concluding remarks

In summary, the evolution of the wavepacket is determined by the instability parameter K. Whatever the sign of K before the slope, a sufficiently large wavepacket tends to form one or more solitons if K increases to a positive value after the slope, and tends to flatten if $K < 0$ after the slope. If K is positive throughout but decreasing in the direction of wave propagation then an initial soliton flattens and disperses. The value of K depends on h/h_1 and $\tau = (2\pi/\omega)\ (g/h_1)^{\frac{1}{2}}$ and on the current. Without current, K increases with h/h_1, but decreases with τ, being zero at $kh = 1.36$.

A steady current exists when $h > h_c$, where h_c is the critical depth, at which $F_1 = 1$. If the flow is positive and subcritical ($0 < F_1 < 1$), then K increases with increasing h/h_1 but decreases with increasing τ. However, if the flow is positive and supercritical ($F_1 > 1$), then K decreases with increasing h/h_1 and τ. Finally, if the flow opposes the wave and is subcritical ($-1 > F > 0$), then K decreases with increasing τ but is not monotonic in h/h_1, having a minimum for some h/h_1. This presents the possibility for soliton fission whether the waves enter the deeper or shallower water. In all cases $K = 0$ when $k(h+\zeta) = 1.36$.

For a strong current over a long distance, bottom friction is important in nature and should be incorporated in future work.

This research has been supported by U.S. National Science Foundation (Grant MEA77-17817A04) and Office of Naval Research (NONR 062-228).

REFERENCES

BENJAMIN, T. B. & FEIR, J. E. 1967 The disintegration of wave trains on deep water. Part 1. *J. Fluid Mech.* **27**, 417–430.

BENMOUSSA, C. 1983 Evolution of surface wave packets over slowly varying depth and current. M.S. thesis, MIT.

CHU, V. H. & MEI, C. C. 1970 On slowly varying Stokes' waves. *J. Fluid Mech.* **41**, 873–887.

DAVEY, A. & STEWARTSON, K. 1974 On three-dimensional packets of surface waves. *Proc. R. Soc. Lond.* **A338**, 101–110.

DJORDJEVIC, V. D. & REDELOPP, L. G. 1978 On the development of a packet of surface gravity waves moving over an uneven bottom. *Z. angew. Math. Phys.* **29**, 950–962.

JOHNSON, R. S. 1973 On the development of a solitary wave moving over an uneven bottom. *Proc. Camb. Phil. Soc.* **73**, 183–203.

MADSEN, O. S. & MEI, C. C. 1969 The transformation of a solitary wave over an uneven bottom. *J. Fluid Mech.* **39**, 781–791.

MILES, J. W. 1980 Solitary waves. *Ann. Rev. Fluid Mech.* **12**, 11–44.

ONO, H. 1974 Nonlinear waves modulation in inhomogeneous media. *J. Phys. Soc. Japan* **37**, 1668–1672.

PEREGRINE, D. H. 1976 Interaction of water waves and currents. *Adv. Appl. Mech.* **16**, 10–117.

SATSUMA, J. & YAJIMA, N. 1975 Initial value problems of one dimensional self-modulation of nonlinear-dispersive waves. *Suppl. Prog. Theor. Phys.* **55**, 284–306.

TAPPERT, F. D. & ZABUSKY, N. J. 1971 Gradient-induced fission of solitons. *Phys. Rev. Lett.* **27**, 1774–1776.

TURPIN, F. M. 1981 Interaction between waves and current over a variable depth. M.S. thesis, M.I.T.

YUE, D. K. P. 1980 Numerical study of Stokes wave diffraction at grazing incidence. Sc.D. thesis, MIT.

YUEN, H. C. & LAKE, B. M. 1980 Instabilities of waves on deep water. *Ann. Rev. Fluid Mech.* **12**, 303–334.

ZAKHAROV, V. E. & SHABAT, A. B. 1972 Exact theory of two-dimensional self-focusing and one-dimensional self modulation of waves in nonlinear media. *Sov. Phys. JETP* **34**, 62–69.